Astronomy & Astrophysics manuscript no. paper111
October 23, 2017

280 one-opposition near-Earth asteroids recovered by the EURONEAR with the Isaac Newton Telescope

O. Vaduvescu[1,2,3,⋆], L. Hudin[4], T. Mocnik[1], F. Char[5], A. Sonka[6], V. Tudor[1], I. Ordonez-Etxeberria[1,7], M. Díaz Alfaro[1,8], R. Ashley[1], R. Errmann[1], P. Short[1], A. Moloceniuc[9], R. Cornea[9], V. Inceu[10], D. Zavoianu[11], M. Popescu[6,12], L. Curelaru[9], S. Mihalea[9], A.-M. Stoian[13], A. Boldea[14,15], R. Toma[16,9], L. Fields[16], V. Grigore[9], H. Stoev[1], F. Lopez-Martinez[1,17], N. Humphries[1], P. Sowicka[1,18], Y. Ramanjooloo[1], A. Manilla-Robles[1], F. C. Riddick[1], F. Jimenez-Lujan[1], J. Mendez[1], F. Aceituno[19], A. Sota[19] D. Jones[2,3], S. Hidalgo[2,3], S. Murabito[2,3], I. Oteo[20,21], A. Bongiovanni[2,3], O. Zamora[2,3], S. Pyrzas[2,3,22], R. Tanausu[2,3], J. Font[2,3], A. Bereciartua[2,3], I. Perez-Fournon[2,3], C. E. Martínez-Vázquez[2,3], M. Monelli[2,3], L. Cicuendez[2,3], L. Monteagudo[2,3], I. Agulli[2,3], H. Bouy[23,24], N. Huélamo[24], M. Monguió[25], B. T. Gänsicke[26], D. Steeghs[26], N. P. Gentile-Fusillo[26], M. A. Hollands[26], O. Toloza[26], C. J. Manser[26], V. Dhillon[27,2], D. Sahman[27], A. Fitzsimmons[28], A. McNeill[28], A. Thompson[28], M. Tabor[29], D. N. A. Murphy[30], J. Davies[31], C. Snodgrass[32], A. H.M.J. Triaud[33], P. J. Groot[34], S. Macfarlane[34], R. Peletier[35], S. Sen[35], T. İkiz[35], H. Hoekstra[36], R. Herbonnet[36], F. Köhlinger[36], R. Greimel[37], A. Afonso[38], Q. A. Parker[39,40], and A.K.H. Kong[41]

(Affiliations can be found after the references)

Submitted to A&A 28 Aug 2017; Re-submitted 10 Oct 2017; Accepted 11 Oct 2017; DOI 10.1051/0004-6361/201731844

ABSTRACT

Context. One-opposition near-Earth asteroids (NEAs) are growing in number, and they must be recovered to prevent loss and mismatch risk, and to improve their orbits, as they are likely to be too faint for detection in shallow surveys at future apparitions.

Aims. We aimed to recover more than half of the one-opposition NEAs recommended for observations by the Minor Planet Center (MPC) using the Isaac Newton Telescope (INT) in soft-override mode and some fractions of available D-nights. During about 130 hours in total between 2013 and 2016, we targeted 368 NEAs, among which 56 potentially Hazardous asteroids (PHAs), observing 437 INT Wide Field Camera (WFC) fields and recovering 280 NEAs (76% of all targets).

Methods. Engaging a core team of about ten students and amateurs, we used the THELI, Astrometrica, and the Find_Orb software to identify all moving objects using the blink and track-and-stack method for the faintest targets and plotting the positional uncertainty ellipse from NEODyS.

Results. Most targets and recovered objects had apparent magnitudes centered around $V \sim 22.8$ mag, with some becoming as faint as $V \sim 24$ mag. One hundred and three objects (representing 28% of all targets) were recovered by EURONEAR alone by Aug 2017. Orbital arcs were prolonged typically from a few weeks to a few years; our oldest recoveries reach 16 years. The O-C residuals for our 1,854 NEA astrometric positions show that most measurements cluster closely around the origin. In addition to the recovered NEAs, 22,000 positions of about 3,500 known minor planets and another 10,000 observations of about 1,500 unknown objects (mostly main-belt objects) were promptly reported to the MPC by our team. Four new NEAs were discovered serendipitously in the analyzed fields and were promptly secured with the INT and other telescopes, while two more NEAs were lost due to extremely fast motion and lack of rapid follow-up time. They increase the counting to nine NEAs discovered by the EURONEAR in 2014 and 2015.

Conclusions. Targeted projects to recover one-opposition NEAs are efficient in override access, especially using at least two-meter class and preferably larger field telescopes located in good sites, which appear even more efficient than the existing surveys.

1. Introduction

The recovery of an asteroid is defined as an observation made during a second apparition (best-visibility period, which typically takes place around a new opposition) following the discovery (Boattini 2000). The recovery of poorly observed asteroids and especially near-Earth asteroids (NEAs) and near-Earth objects (NEOs) is a very important task to prevent object loss and mispairing, and to improve the orbits and dynamical evolution.

Very few papers have so far described targeted recovery and follow-up programs of NEAs. We mention here the pioneering efforts of Tatum (1994), who used three telescopes in Canada (including the DAO 1.85 m) to follow up 38 NEAs and recover 2 NEAs during 1992. Boattini (2000) presented some statistics based on a sample of multi-opposition NEAs, sorting recoveries into four classes that included new observations and data mining of existing image archives and concluding that planning telescope observations is the best way to recover NEAs. Tichá (2000) and Tichá (2002) presented recoveries of 21 NEAs over four and half years (1997-2001) using the 0.57 m telescope at Klet' observatory in Slovakia. Since 2002, the follow-up (mainly) and recovery efforts at Klet' have been improved through the KLENOT program, using a dedicated 1.06 m telescope equipped with a 33′ square camera. Over six and half years (2002-2008), this program counted more than 1000 NEA follow-up observations, but only 16 NEA recoveries (Tichá 2009), suggesting that larger (preferably at least 2 m class) and larger field facilities are needed today for recovery.

During the past few years, recovery of poorly observed NEAs has become essential to confirm the orbits of one-opposition objects that have not been observed for years since discovery and very short follow-up (typically only a few weeks),

⋆ email: ovidiu.vaduvescu@gmail.com

some in danger of loss or mispairing with newly discovered NEAs.

Particular attention should be given when telescope time is scarce, requiring a larger aperture, field of view, and mandatory quality control of the astrometry and orbital fitting. Within the European Near Earth Asteroids Research (EURONEAR) (Vaduvescu 2008), follow-up and recovery have been the main astrometric tools used for the orbital amelioration of NEAs, potentially hazardous asteroids (PHAs), and virtual impactors (VIs) (Birlan 2010; Vaduvescu 2011, 2013).

Since 2000, A. Milani and his Pisa University team have improved the uncertainty models needed to search for poorly observed asteroids (one-opposition with short arcs, or asteroids that have not been observed for many years), considering nonlinear error propagation models to define the sky uncertainty area, which typically spans an elongated ellipse (Milani 1999a, 2010). It is essential to use these theories to recover one-opposition NEAs, and this could be easily done today using the ephemerides given by the NEODyS server[1] or the OrbFit Software Package[2].

When we count the entire NEA database as of Aug 2017 (about 16,500 objects with orbital arcs expressed in days), about 50% represent one-opposition NEAs (more than 8000 objects), and this percentage is growing because of the accelerated discovery rate of existing and future surveys. A pool of about 400 one-opposition NEAs (5%) brighter than $V < 24$ mag with solar elongation greater than 60° are recommended for observations at any particular time by the Minor Planet Centre (MPC) at any particular time in their Faint[3] and Bright[4] NEA Recovery Opportunities lists. Around opposition, many of these targets escape detection by major surveys because they are faint, because the visibility windows are relatively short, because of fast proper motions, and because of bright Moon and Milky Way interference.

In 2014, we started a pilot recovery program with the aim to observe 100 one-opposition NEAs using the 2.5 m Isaac Newton Telescope (INT) accessed during at most 30 triggers (maximum one hour each available night) through the Spanish TAC ToO time (Target of Opportunity or override mode). This program produced some promising results (about 40 recoveries during only 15 triggers), nevertheless, some visibility windows were lost because telescope access was constrained to only during the allocated Spanish one-third fraction, only when the imaging camera was available, and only during dark time. During the next three semesters, we multiplied the trigger windows by proposing the same program to the other two TACs (UK and Dutch), who have agreed to share the load and granted 15-20 h each during each of the next three semesters, but mostly in “soft” mode (only at the discretion of the observer) and also accepting some twilight time (20 min mostly before morning) so that their own research was not strongly affected. The first semester in 2016 concluded with the last Spanish allocation, and by mid-2016, we reached the goal of recovering more than half of the one-opposition NEAs recommended for observation by the MPC.

In this paper we report the achievements of this project, discussing the observing methods and findings, and comparing the INT with other facilities used for similar projects. In Section 2 we present the planning tools and observations. The data reduction software and methods are included in Section 3, the results are presented in Section 4, and we conclude in Section 5.

[1] http://newton.dm.unipi.it/neodys/index.php?pc=0
[2] http://adams.dm.unipi.it/orbfit
[3] http://www.minorplanetcenter.net/iau/NEO/FaintRecovery.html
[4] http://www.minorplanetcenter.net/iau/NEO/BrightRecovery.html

2. Planning and observations

Here we present the tools we used for planning, the facilities, and the observing modes.

2.1. Recovery planning tool

In April 2010, the “One-opposition NEA Recovery Planning” tool[5] was written in PHP by Marcel Popescu and Ovidiu Vaduvescu to assist in planning the observations of the one-opposition NEAs retrieved from the Faint and Bright Recovery Opportunities for NEOs MPC lists. The input is the observing night (date) and start hour (UT), the number of steps and time separator (typically 1h), selection of the bright or faint MPC lists, the MPC observatory code, the maximum observable magnitude for the targets, the minimum altitude above horizon, the maximum star density in the field (to avoid the Milky Way), the maximum proper motion, and the maximum positional uncertainty (one sigma) as retrieved by the NEODyS server. The output consists of a few tables (one for each time-step), prioritizing targets based on a few observability factors to choose from, such as the apparent magnitude, altitude, proper motion, sky plane uncertainty, or taking them all into account at once. Other data listed in the output are the stellar density, the angular distance to the Moon, and the Moon altitude and illumination.

2.2. INT override observations

The 2.5 m Isaac Newton Telescope (INT) is owned by the Isaac Newton Group (ING). It is located at 2336 m altitude at the Roque de los Muchachos Observatory (ORM) on La Palma, Canary Islands, Spain. The mosaic Wide Field Camera (WFC) is located at the $F/3.3$ INT prime focus, consisting of four CCDs with 2048×4098 13.5 μm pixels each, resulting in a scale of 0.33″/pixel and a total 34′ square field with a missing small square 12′ in its NW corner. During all runs, we used the Sloan r filter, which suppresses fringing and improves the target signal-to-noise ratio (S/N) in the twilight. The telescope is capable of tracking at differential rates, and we mostly used tracking at half the NEA proper motion in order to obtain a similar measurable trailing effect for both the target and reference stars. The INT median seeing is 1.2″ , and we typically required an ORM seeing monitor limit of 1.5″ in order for the triggers to become active.

In Table 1 we include the observing proposals (all three TACs), the number of executed triggers (in bold), and the total granted number of triggers (e.g., **15**/30 means that 15 triggers were executed of a maximum allowed 30). Additionally, available fractions during another nine ING discretionary nights (“D-nights”) were used to observe a few dozen targets, involving some ING student observers. In total, about 130 INT hours were used for this program. All the observers were invited to become coauthors of this paper.

For each target field, typically 6-8 consecutive images (up to 15 for very faint targets) were acquired with exposures of typically 60-90 s each (up to a maximum 180 s in a few cases), so that the trail effect would not surpass twice the seeing value. Considering the WFC readout time (49 s in the slow and 29 s in the fast mode used mostly in this project), one target sequence could take between 10 and 20 minutes, which means that we could accommodate between three and six targets during a one-hour typical override. For targets with larger uncertainties

[5] http://www.euronear.org/tools/planningmpc.php

Table 1. Observing proposals and number of triggers activated (in bold) with the Isaac Newton Telescope (INT)

Semester	SP TAC		UK TAC		NL TAC	
2014A	136-INT09/14A (C136)	**15**/30				
2014B	088-INT10/14B (C88)	**6**/20	I/2014B/02 (P2)	**10**/20		
2015A	033-MULT-2/15A (C33)	**9**/20	I/2015A/05 (P5)	**1**/20	I15AN003 (N3)	**3**/20
2015B	001-MULT-2/15B (C1)	**14**/15	I/2015B/02 (P2)	**11**/15	I15BN001 (N1)	**4**/15
2016A			I/2016A/02 (P2)	**6**/10		

($3\sigma \gtrsim 600''$), we observed two or three nearby fields that covered more than one degree along the line of variation.

2.3. Other telescopes

In addition to the INT override program, three other telescopes accessible to EURONEAR were used to recover a few targets and a few NEA candidate discoveries for a very limited time (about 10 h in total). The first was the 4.2 m F/11 William Herschel Telescope (WHT) at ORM equipped with the ACAM imaging camera (circular 8′ field) during two D-nights testing and twilight time, and another four nights when the current observer had his targets at very high airmass. The second was the ESA 1 m F/4.4 Observing Ground Station (OGS) equipped with a 45′ square field camera at Tenerife Teide Observatory, used during two nights for the recovery of two target NEAs and to secure three of our NEA incidental discoveries. Additionally, a third telescope was used to follow up a few NEA candidate discoveries, namely the Sierra Nevada Observatory 1.5 m (T150) F/12.5 with the CCDT150 camera 8′ square field.

Table 2 lists the observing log, which includes all the 457 observed fields (437 using the INT, 12 using the WHT, and 4 using the OGS). We ordered this table based on the asteroid designation (first column), then the observing date (start night), listing the apparent magnitude V (according to MPC ephemerides), the proper motion μ and the positional uncertainty of the targets (as shown on the observing date by MPC at 3σ level), the number of acquired images (including nearby fields), and the exposure time (in seconds). In the last three columns we list the current (Jul 2017) status of the targets (to be discussed next), the MPS publication that includes our recovery, and some comments that can include the PHA classification, other used telescopes (WHT or OGS), the track-and-stack technique (TS, whenever used), and other possible external stations (MPC observatory code) and the date of later recovery (given only for later recoveries when we were unable to find the targets or for joined simultaneous recoveries).

3. Data reduction

We present next the data reduction software and quality control methods used to find and measure the targets. Three steps were performed during the day following observations: the image reduction and field correction (by one person), the visual search and measurement of the target and all other moving objects (known or unknown) appearing in each field (distributing the work to a team of a few people), and finally the quality control and reporting of all data to MPC (by the project leader).

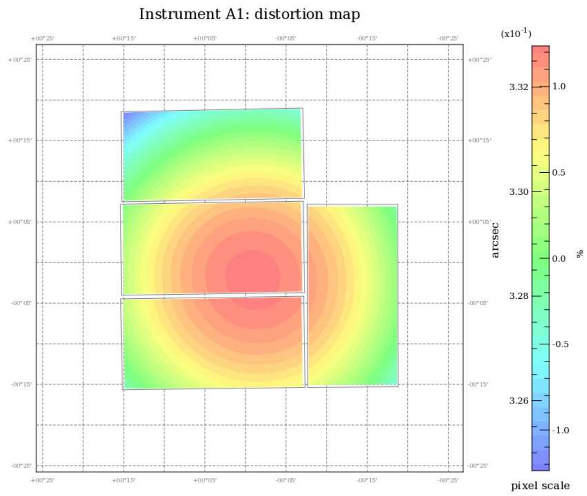

Fig. 1. Typical THELI field distortion of the INT-WFC field.

3.1. THELI

Very accurate astrometry (comparable to or lower than the reference star catalog uncertainty, preferably below $0.1''$) is essential to correctly link and improve the orbits that have been poorly observed in the past, like one-opposition NEAs. Any fast system and prime focus larger field camera (such as INT-WFC) provides quite distorted raw astrometry that needs correction in order to be used for accurate measurements. We used the GUI version[6] of the THELI software (Erben 2005; Schirmer 2013) to reduce the raw WFC images using the night bias and flat field and to resolve the field correction to all four CCDs in each WFC-observed field by using a third-degree polynomial distortion model. In Figure 1 we include one typical field distortion map output of THELI (running Scamp), showing pixel scale differences of up to $0.006''$ between the center and corners of the WFC field, which can produce errors of up to $40''$when a simple linear astrometric model is applied. For most of the data reduction, we used the PPMXL reference star catalog (Roeser 2010), while UCAC4, SDSS-DR9, or USNO-B1 were used when the field identification failed because of a lack of stars or small dithering between frames.

3.2. Astrometrica

The Windows Astrometrica software[7] is popular among amateur astronomers for field registering, object identification, and astrometric measurement of the asteroids; it is written by the Austrian amateur astronomer Herbert Raab. We used it after every run, up-

[6] https://www.astro.uni-bonn.de/theli/gui/index.html
[7] http://www.astrometrica.at

dating the MPCORB database to take all newly discovered asteroids and updated orbits into account. In 2014, Ruxandra Toma and Ovidiu Vaduvescu wrote a user guide manual[8] (21 pages) aimed for training the new members of the reduction team.

3.2.1. Classic blink search

We used Astrometrica for each observed WFC field to independently blink the four CCDs, identifying all moving sources (as known or unknown asteroids), and measuring them. Typically, between one and two hours were spent by one reducer for each WFC field. Although Astrometrica is capable of automatic identification of moving sources, given the faintness of our NEA targets, we decided to use visual blink and manual measurements. In addition to the targeted NEA, typically up to a few dozen main-belt asteroids (MBAs, about half of them known and half unknown) could be identified in good seeing conditions in each observed WFC field.

3.2.2. Track-and-stack

When the NEA target could not be seen using the classic blink search, then the Astrometrica track-and-stack method ("TS") was used, either with the "median" option to eliminate most of the stars, or with the "add" option to improve the detection of extremely faint targets (S/N=2-3). The linear apparent motion assumed by the TS procedure could be affected by the diurnal paralax effect, and the TS detection could fail during very close flybys or/and a longer observing time that was affected by diurnal effects, but we consider that none of our targets was affected by these circumstances, as the length of each observing sequence was short. To limit the search area, we developed a method using DS9 to load the Astrometrica TS image and overlay the NEODyS 3σ uncertainty, thus restraining the visual search to a very thin ellipse area (possible to save and load as a DS9 region) typically passing across the central CCD4 (holding the target most of the time) or/and nearby CCDs or fields. We include in Figure 2 one typical DS9 overlay (NEA 2012 EL5 on 23 Aug 2015 with uncertainty $3\sigma = 788''$ prolonging to the nearby CCD2), which allowed the identification of the target falling exactly on the major axis of the NEODyS uncertainty ellipse overlaid on the stack of 6×60s individual images.

3.3. Quality control

Astrometrica can easily identify moving sources with well-known asteroids (observed at two oppositions at least) by calculating their ephemerides using an osculation orbit model with orbital elements very close to the observing time, which provides a very good accuracy of $\sim 1''$. After each observing night, we used Astrometrica to check all moving sources that were visible in each WFC field against known MBAs included in the updated MPCORB database[9]. Nevertheless, one-opposition objects and especially NEAs closer to Earth are affected by positional uncertainties, and they should be checked using additional tools.

[8] http://www.euronear.org/manuals/Astrometrica-UsersGuide-EURONEAR.pdf

[9] http://www.minorplanetcenter.net/iau/MPCORB.html

3.3.1. AstroCheck, FITSBLINK, and O-C calculator

In 2015, Lucian Hudin developed the EURONEAR PHP tool AstroCheck[10] to verify the consistency of all astrometric measurements obtained in each WFC field (known or unknown asteroids). This tool assumes that a simple linear regression model holds for relatively short and contiguous observational arcs like those observed during 10-20 min runs for each target of our recovery project. A maximum error (default $0.3''$ consistent with WFC pixel size) is allowed, all other outliers being flagged in red, these positions being revised or discarded by the reducer.

We used the server FITSBLINK[11] , which identifies known objects and provides tables and plots to check the $O - C$ (observed minus calculated) residuals for all asteroids (mostly MBAs) identified by Astrometrica in each WFC field. The calculation of the asteroid positions is based on osculating elements near the current running date, so the identification is correct for checks after each observing run, but it could fail for older measurements. The great majority of the residuals are scattered around the origin in the $\alpha - \delta$ FITSBLINK plots, proving the correct identification of the MBAs. Some asteroids (MBAs and target NEAs) show normal non-systematic clustering around values different than zero (typically by a few arcseconds), suggesting the correct identification of poorer known orbits. If any object presents systematic O-C residuals (typically located far from the origin), then this most probably represents an erroneous identification, and FITSBLINK flags these objects as unknown.

In addition to FITSBLINK, to check MBAs residuals, we used the EURONEAR tool O-C Calculator[12] , which provides tables to check for accurate residuals for each target NEA. The residuals are calculated based on accurate ephemerides run using the OrbFit planetary perturbation model that is automatically queried via NEODyS[13]. Each correctly identified one-opposition NEA target must show normal non-systematic scatter (located around a center different than the origin), otherwise the identification is false.

For the target NEAs, the FITSBLINK and the O-C Calculator residuals could be randomly spread (non-systematic) around a point which may be different than the origin, while for most MBAs, the O-C values are typically spread around the origin.

3.3.2. Find_Orb and Orbital Fit

The Find_Orb software[14] is a user-friendly popular orbit determination software under Windows or Linux for fitting orbits of solar system objects based on existing observations, written by the US American amateur astronomer Bill Gray. We used Find_Orb to finally check NEA targets that showed larger positional uncertainties. Past observations were downloaded from the MPC Orbits/Observations database[15], which was updated with our proposed identification and astrometric measurements, before using Find_Orb in two steps.

First, using only past positions, an orbit is fit in a few (typically 3-4) converging steps by activating all perturbers and rejecting outlier measurements greater than $1''$ in α or δ. Virtually all fits should produce an overall σ root-mean-square deviation smaller than $1''$. Second, we append our measurements to the input observation file to load in Find_Orb to attempt an improved

[10] http://www.euronear.org/tools/astchk.php

[11] http://www.fitsblink.net/residuals

[12] http://www.euronear.org/tools/omc.php

[13] http://newton.dm.unipi.it/neodys

[14] https://www.projectpluto.com/find_orb.htm

[15] http://www.minorplanetcenter.net/db_search

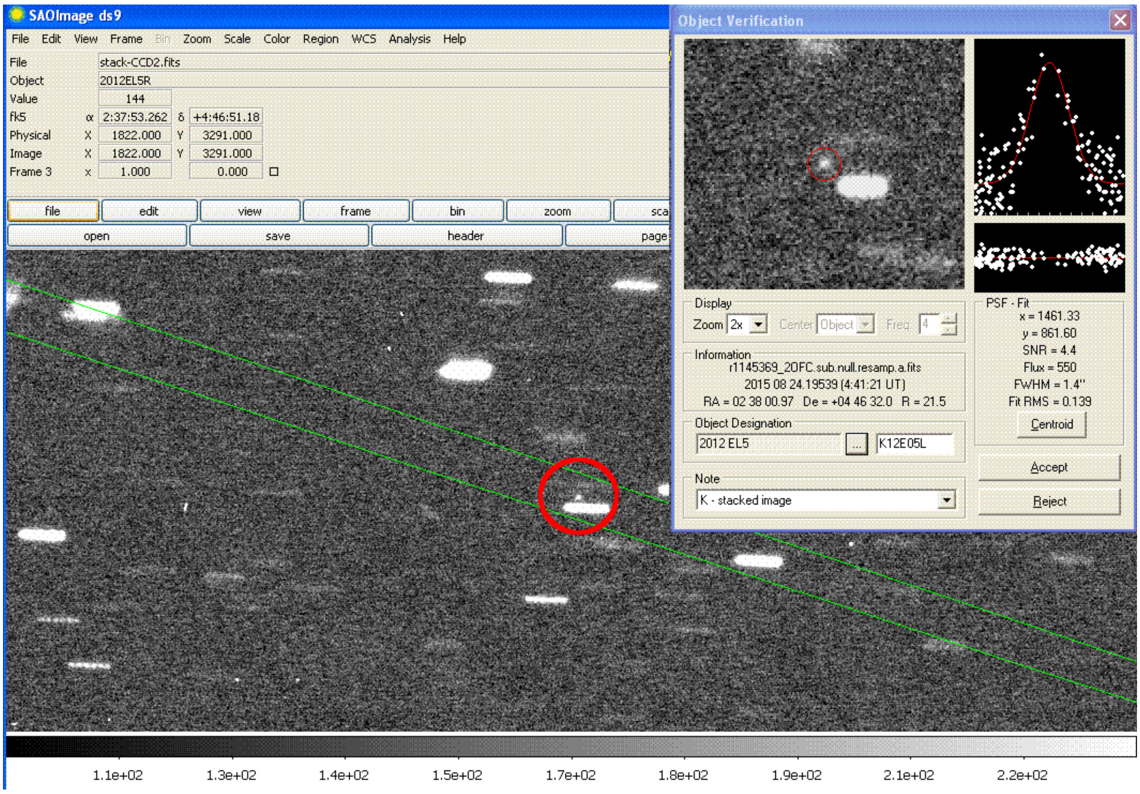

Fig. 2. Track-and-stack Astrometrica image (composition of six individual images using the "add" option) overlaid on DS9 the NEODyS uncertainty ellipse (green) that we used to find the target NEA (2012 EL5, circled in red).

orbital fit in a few (3-4) converging steps, which must conserve or slightly improve σ (typically by $0.01-0.02''$) and show random distributions in both α and δ (typically below $0.3''$ in module) around zero for our measurements.

If any target presents a systematic $O-C$ trend or increases the σ orbital fit, then the identification is false or the candidate (typically very faint or found using the TS technique) represents an artifact and is discarded.

4. Results

4.1. Targeted NEAs

We accessed time for the NEA recovery program during 102 nights: 94 nights using the INT (mostly in override mode for a maximum of 1 h each night and using some D-nights), plus another 6 nights using the WHT and 2 nights using the OGS. We targeted 368 one-opposition NEAs (including 56 PHAs), observing 453 fields: 437 with the INT (representing 96% of the program), 12 with the WHT, and 4 fields with the OGS. We recovered 290 NEAs in total (79% from all 368 targets), of which 280 targets were recovered with the INT. One hundred and three recovered objects (representing 28% of all targets) were observed at second opposition only by EURONEAR, proving the importance of planned recovery compared with shallower surveys.

Orbital arcs were typically prolonged from a few weeks to a few years, our oldest one-opposition recoveries improving orbits of objects that were not seen for up to 16 years (1999 DB2 and 1999 JO6). Based on Table 2, the user can evaluate the extended arc (in years) by simply subtracting the discovery year (first four digits in the first column NEA designation) from the observing date (first four digits standing for the year), the oldest recoveries being included in the first part of the table.

Because they were not recovered during the first attempt, 67 NEAs (18%) were targeted multiple (typically two to three) times, some of them even up to six times (2008 ON, resolved during four nights), in order to secure recoveries of very faint objects that were seen only with TS and to minimize the risk of false detections.

We sorted our findings into a few groups that we list in Table 2 under the Status column:

- REC - recovery (followed by other stations);
- RECO - recovery only (not followed by others);
- RECJ - recovery joined (simultaneously with others);
- RECR - revised recovery (in 2017 or following other later recovery);
- NOTF - not found (but found by others later);
- NOTFY - not found yet (by any other station).

We were unable to find 79 objects (21% of all 368 targets) that are marked with status NOTF or NOTFY in Table 2 for several reasons, the most common being that some targets were fainter than originally predicted, others were affected by cirrus, calima, or late twilight, and a few were hidden by bright stars or have fallen in the WFC gaps. Of these, 46 objects (12%) were recovered later by other programs or surveys (status NOTF), and another 33 objects (9%) have not been found yet (by July 2017); these are marked with the status NOTFY. Additionally, we were able to recover 16 objects later (status RECR), following a revised search (carried out in 2017) based on an orbit that was improved by other programs. Here we report the most efficient programs (MPC code, facility, and number of later recoveries missed by us): 568+T12 (CFHT and UH telescopes, 28 recoveries or 7% of all our targets), 926 (Tenagra II, 9 recoveries), J04 (ESA/OGS Tenerife, 8), F51 (Pan-STARRS 1, 6),

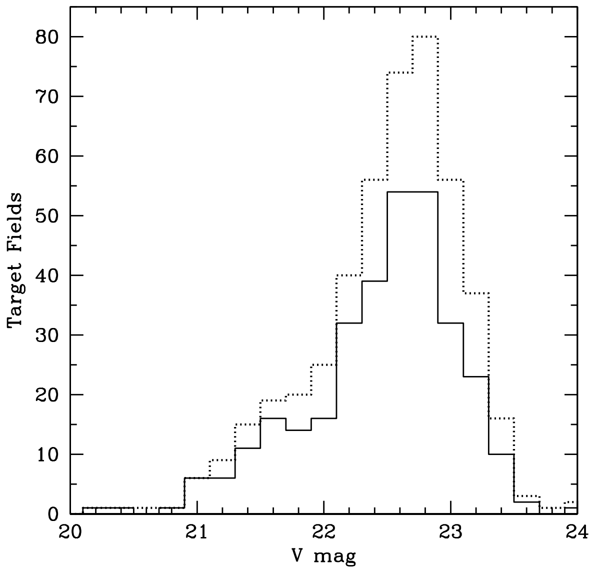

Fig. 3. Distribution of the NEA apparent magnitude.

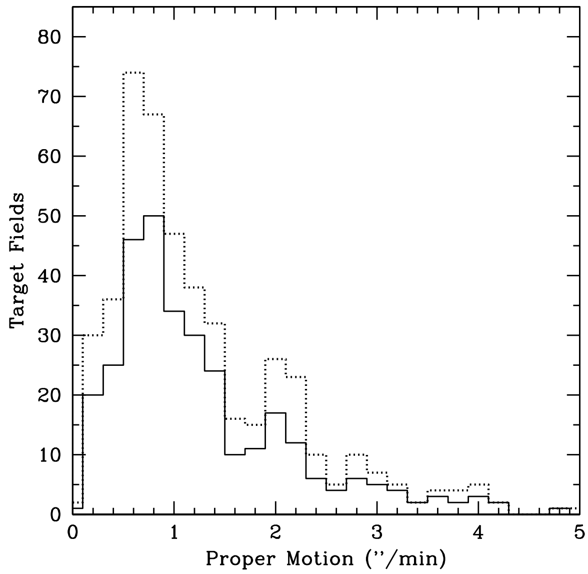

Fig. 4. Distribution of the NEA proper motion.

807+W84 (CTIO and Blanco/DECam, 5), 291 (Spacewatch II, 4), H21 (ARO Westfield, 4), 705 (SDSS, 3), G96 (Catalina, 2), 695 (KPNO, 2), 033 (KSO, 2), H36 (Sandlot 2), 675+I41 (Palomar and PTF, 2), 309 (Paranal VLT, 1), G45 (SST Atom Site, 1), and T08 (ATLAS-MLO, one recovery).

In Figure 3 we present the magnitude distribution of all targeted fields (plotted with a dotted line) and recovered targets (solid line). Most targets had $V \sim 22.8$, and most targets were also recovered around $V \sim 22.8$. A few fainter objects were targeted and some were recovered close to $V \sim 24.0$ using the TS technique.

In Figure 4 we present the proper motion distribution of all targeted fields (dotted line) and recovered targets (solid line). Most targets had relatively small proper motion (around $\mu \sim 0.7''$/min, sampling the morning small solar elongation targets), while another small peak is visible around $\mu \sim 2.0''$/min and other faster objects (up to $\mu \sim 5.0''$/min) sample closer flybys and opposition apparitions.

In Figure 5 we present the 3σ positional uncertainty distribution of all targeted objects (dotted line) and recovered targets (solid line). Most targets had $3\sigma < 1000''$ (due to the selection limit), and there were 20 targets with uncertainties of up to $3000''$ (outside the plot) for which we observed two or three nearby fields.

Figure 6 plots the histogram counting all the observed fields (upper dotted line) as a function of the ecliptic latitude (β), showing that most fields were observed between $-20° < \beta < +50°$. The recovered targets are plotted with a continuous line (in the middle), and the one-night recoveries are plotted with a dashed line (in the bottom). They are discussed in Section 4.2.

Figure 7 plots the O-C residuals (observed minus calculated) for 1,854 NEA measurements from the NEODyS database based on the improved orbits (by 3 Aug 2017). Most of the points are located around the origin, with a standard deviation of $0.26''$ in α and $0.34''$ in δ. Only eight points (0.4% of all data) sit outside $1''$ in either α or δ; they represent measurements of very faint targets.

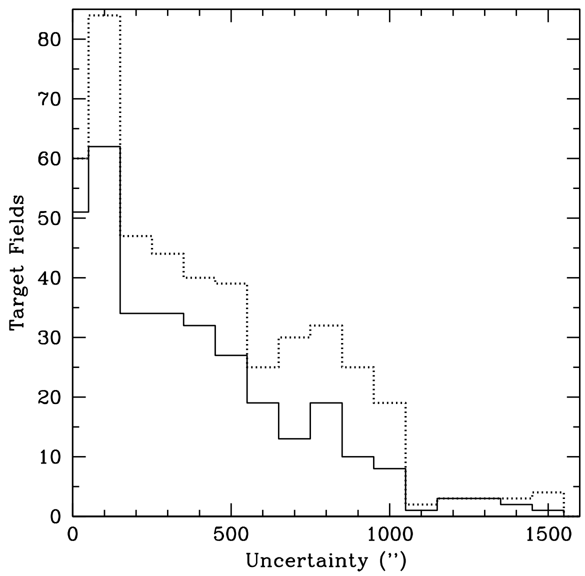

Fig. 5. Distribution of the NEA 3σ uncertainty.

4.2. Main-belt asteroids and the NEA misidentification risk

All moving sources found through blinking in the WFC images were identified with known asteroids or were labeled as unknown asteroids and reported to MPC promptly after each run (typically during the next day). By checking the MPCAT-OBS and the ITF archives[16], we were able to count about 22,000 observations of about 3,500 known minor planets (mostly MBAs) and about 10,000 observations of about 1,500 unknown objects (most consistent with MBAs) reported by our team between Sep 2013 and Oct 2016 as part of this project.

In a series of papers, A. Milani and colleagues proposed new algorithms to better approximate and predict the recovery region of poorly observed asteroids and comets by using a nonlinear

[16] http://www.minorplanetcenter.net/iau/ECS/MPCAT-OBS/MPCAT-OBS.html

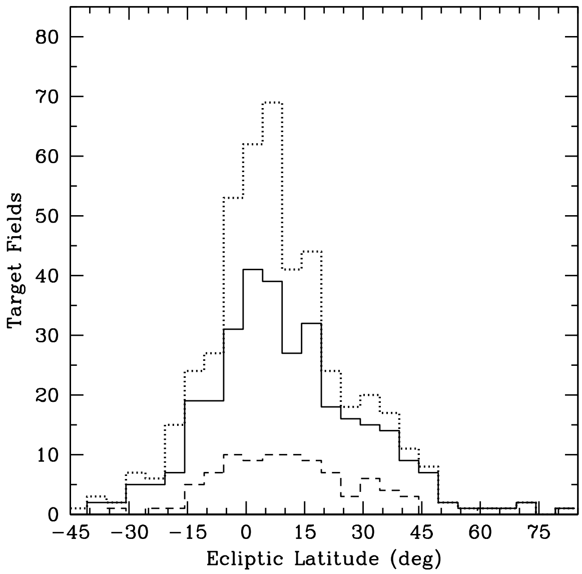

Fig. 6. Distribution of the NEA ecliptic latitudes.

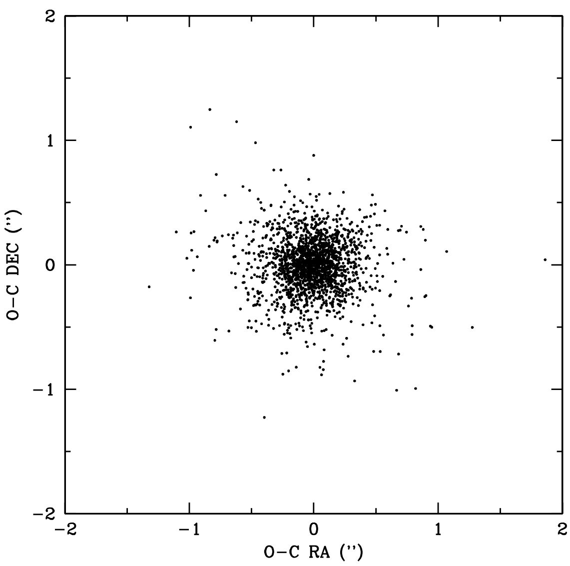

Fig. 7. O-C residuals for 1,854 positions of 368 one-opposition NEAs.

theory to compute confidence boundaries on the modified target plane (Milani 1999a,b, 2000, 2001). This theory was implemented in NEODyS, which has been used by us to plot the uncertainty regions of the one-opposition NEA targets, which is essential for a correct identification of very faint asteroids (found with the TS techique) and one-night recoveries. We have made 91 one-night recoveries (counted by Aug 2017), meaning that targets were identified and measured during only one night as part of our NEA recovery project (neither by us during another night, nor by others until Aug 2017). There is some risk for misidentification in these cases when some targets fall in a dense ecliptic field populated with MBAs. To assess this risk, in Figure 6 we show the ecliptic latitude distribution by plotting all target fields (upper dotted line), the recovered target fields (middle solid line), and one-night recoveries (bottom dashed line). When we counted the recoveries close to the ecliptic ($-5^\circ < \beta < +5^\circ$), we found 19 risk cases (20% of all one-night recoveries) when target NEAs might be confused with MBAs moving at similar direction and rate. The following five precaution measures (adopted for most observed fields) minimize false detections in these cases:

- We detected all known moving objects and identified all know MBAs and other possible known NEAs in all fields.
- We ensured that O-Cs for the NEA candidate detections were non-systematic (they might spread around a point different than zero, but should not show any systematic trend).
- We plotted the predicted NEODyS uncertainty regions for the target NEAs, ensuring that each candidate NEA detection falls very close to (typically within 1″) the long axis of the NEODyS uncertainty ellipse.
- We fit each candidate detection (positions) to the existing orbit, downloading old observations from the MPC database and using Find_Orb to fit the improved orbit, ensuring that the orbital RMS remains the same or improves slightly (typically by 0.01 – 0.02″) after the fit and that our candidate positions O-Cs are non-systematic and spread around zero in the new orbital fit.
- We ensured that our measured magnitudes of all targets were similar to their predicted magnitudes (typically within 1 mag, allowing for the unknown color index $r - V$, for some errors in the magnitudes, and for a higher amplitude light-curve that might be due to more elongated objects).

Using all these checks, we reduced the risk to confuse any one-night target NEA with other MBAs. This is supported by many other one-night recoveries that were confirmed later by other stations (marked with REC or RECJ in Table 2).

4.3. New serendipitous INT NEA discoveries

Vaduvescu (2015) reported the first EURONEAR NEA discoveries from La Palma that were serendipitously found as unknown fast-moving objects in some INT WFC fields taken in 2014 as part of the present one-opposition NEA recovery project. Here we present discovery circumstances of four other secured NEAs in 2015, plus two other probably lost NEOs, together with their composite images shown in Figure 8. In total, EURONEAR discovered and secured nine NEAs in 2014 and 2015, the only such findings from La Palma and using the INT.

4.3.1. 2015 HA117

The very fast 15″/min and relatively faint $R \sim 22$ mag NEA candidate EUHI640 was discovered by Lucian Hudin on 23/24 Apr 2015 in the one-opposition WFC field of NEA 2003 WU153 observed by Matteo Monelli and Lara Monteagudo (MPS 603500). Thanks to the INT override access, the object was recovered the next night by the same team, who scanned 25 WFC fields spanning the MPC uncertainty area, then by the INT, and four days later, it was caught by the VLT close to the South celestial pole (MPS 604697). It became 2015 HA117, estimated at $H = 27.2$ and with a size of 10-24 m, apparently having an Amor orbit with $MOID = 0.01832$ a.u. (based on a seven-day arc), and has remained unobserved since then.

4.3.2. 2015 LT24

The fast 8″/min EUVI053 $R \sim 21.3$ mag NEA candidate was discovered by Victor Inceu in images taken on 14/15 Jun 2015

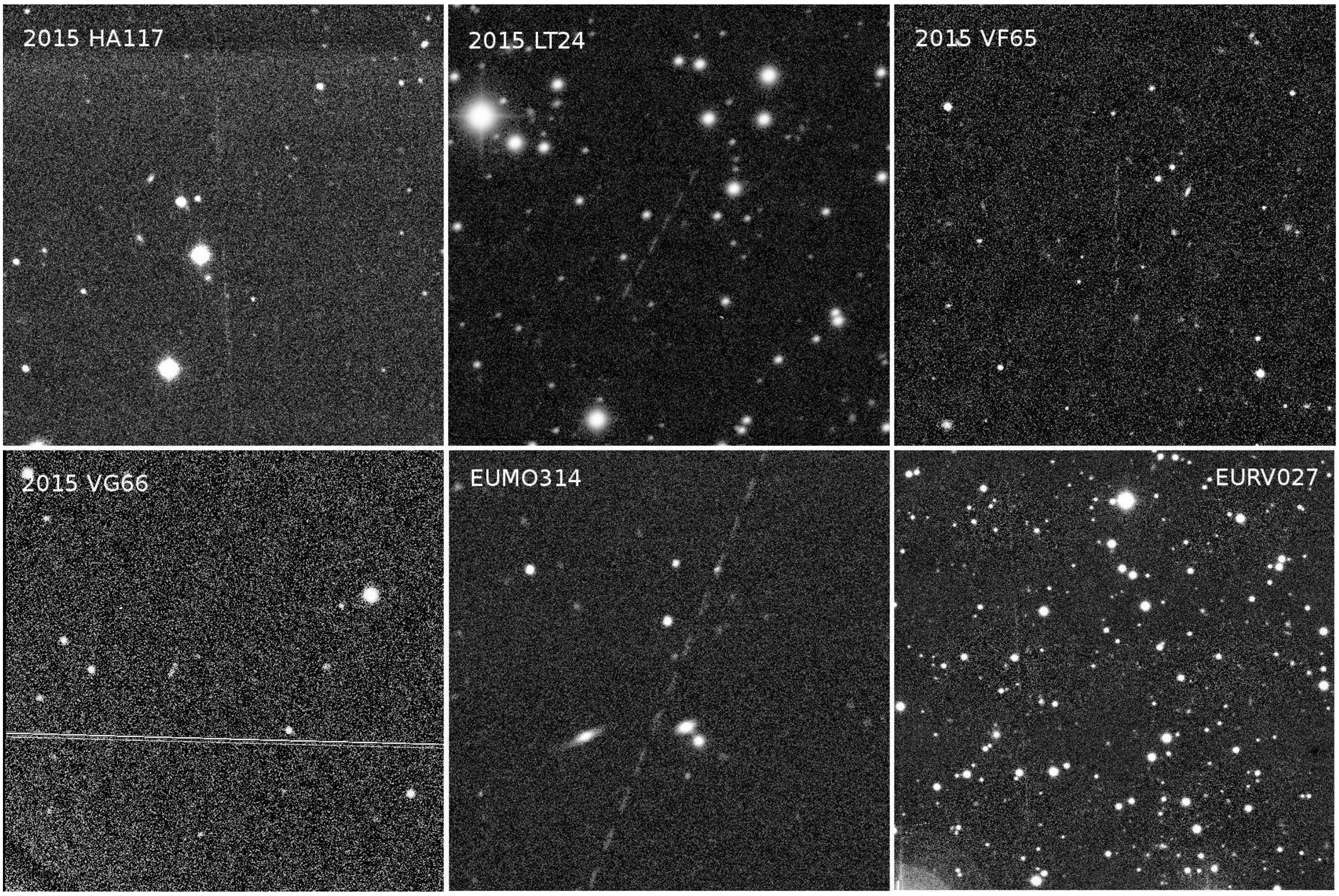

Fig. 8. Composite images of the six serendipitous NEA discoveries (four secured and two lost objects) by EURONEAR using the INT in 2015. Crops are in normal sky orientation (north is up, east to the left), $3' \times 3'$ field of view, except for EURV027, which is barely visible as three very long vertical trails at the left of the $6' \times 6'$ field.

by Stylianos Pyrzas, who chased the known one-opposition 2012 HO2 NEA (MPS 611632). It was saved during the next night with the INT by the same team, then followed-up by other telescopes related to EURONEAR (OGS 1 m and Sierra Nevada 1.5 m), which prolonged its arc to 11 days. Designated as 2015 LT24, it is a relatively large $H = 22.4$ 100-220 m Apollo object with $MOID = 0.15616$ a.u.

4.3.3. 2015 VF65

EUHV001 was another very fast (11″/min) $R \sim 22$ mag NEA candidate discovered as a trailing object by Lucian Hudin on 7/8 Nov 2015, searching for the one-opposition target 2010 VC72 (right field) observed by Odette Toloza (MPS 645818). Thanks to the NEOCP posting, it was saved on next night by Spacewatch and the OGS 1 m and became 2015 VF65, which was followed-up with the INT and another station later (13 day arc). This resolved into an Apollo orbit with an $MOID = 0.05225$ a.u. and $H = 26.1$, corresponding to a size of 18-40 m.

4.3.4. 2015 VG66

EUHV002 was a moderate NEA candidate ($\mu = 1.6''$/min) relatively bright $R = 19.4$ mag, first seen on 8/9 Nov 2015 by our most prolific discoverer Lucian Hudin in one of the 15 chasing fields (EUHV001I) that were taken by Odette Toloza to secure our previous NEA candidate (MPS 645822). Despite its relatively modest MPC NEO score (42%), we decided to chase it because of its location above the NEA border on the $\epsilon - \mu$ plot (Vaduvescu 2011). On the next night, it was secured by the INT observers Odette Toloza and Christopher Manser, then precovered in Pan-STARRS images by Peter Veres (private communication), and later observed by other stations (18-day arc). It has an Apollo orbit with an $MOID = 0.01991$ a.u. and $H = 23.2$, corresponding to a quite large object of 72-161 m.

4.3.5. EUMO314

This very fast NEA candidate ($\mu = 15''$/min, $R \sim 19.3$ mag) was seen by Teo Mocnik in 15 images taken on 1/2 Mar 2015 by Fatima Lopez while chasing another faint NEA candidate (EUMO311). It was lost, unfortunately, the WFC being replaced on next morning by the IDS spectrograph, while no other station could save it.

4.3.6. EURV027

This extremely fast NEO candidate ($\mu = 40''$/min) was seen by Ovidiu Vaduvescu as four very faint (probably $R \sim 23$ mag) and long trails in images taken on 14/15 Aug 2015 by Joan Font in the 2013 VM4 target field. This should correspond either to a very small (a few meter) object close to opposition or more likely a tiny geocentric object (Gareth Williams, private communication). It is barely visible in Figure 8 as three vertical very long trails on the left side of the composite image.

4.3.7. Other NEA candidates

About 15 other slower ($\mu < 1.5''$/min) and sometimes extremely faint ($S/N < 5$) NEA candidates were found in some other fields scanned by our program. Most of them were chased with the INT on the next nights, and we posted some on the NEOCP list. Many of them could not be recovered (even going deeper with the INT), suggesting that they are artifacts, while others were recovered and were found to be MBAs or close NEA species. We note the following: EUHV056 - a probable Jupiter Trojan (65%, according to MPC), 2014 RC13 (EUMO201) - Jupiter Trojan (MPO 311499), 2015 QT4 (EURV028) - Hungaria (MPO 382801), and 2014 LP9 (EUHT164) - Mars crosser (MPO 300699).

5. Conclusions

A project for recovering one-opposition NEAs recommended by the MPC was carried out during a fraction of 102 nights (~ 130 hours total) between 2013 and 2016 using the INT telescope equipped with the WFC camera. We accessed this time as part of ten proposals with time awarded by three committees mostly in soft-override mode and accepting some twilight time, plus other available time during a few D-nights. The data were rapidly reduced (typically during the next day) by a core team of about ten amateurs and students led by the PI, who checked and promptly reported all data to the MPC. We outline the following achievements:

- We targeted 368 one-opposition NEAs (including 56 PHAs) for which we observed 437 WFC fields with the INT.
- We recovered 290 NEAs (79% from all targets), sorted into four groups (REC, RECO, RECJ, and RECR), the majority with the INT (280 targets).
- Most targets and recovered objects have magnitudes centered around $V \sim 22.8$ mag (typically recovered through blink), while some are as faint as $V \sim 24$ mag (only visible with track-and-stack and search in the uncertainty ellipse).
- One hundred and three objects (28% of all targets) have been recovered only by EURONEAR (but no other survey, until Aug 2017 at least).
- Orbital arcs were prolonged typically from a few weeks to a few years, our oldest recoveries improving orbits of objects that have not been seen for up to 16 years.
- Sixty-seven NEAs (18%) could not be found during a first attempt, and they were targeted multiple (typically two to three) times.
- Forty-six objects (12% of all targets) were not found, but were recovered later by other programs or surveys (UH+CFHT 7%, Tenagra, ESA OGS, and major surveys less than 2% of our targets each).
- Most targets were slow ($\mu \sim 0.7''$/min sampling the morning small solar elongation targets), others concentrated around $\mu \sim 2.0''$/min, while others are faster (up to $\mu = 5.0''$/min).
- Given the WFC $34'$ field, our selection limit in positional uncertainty was $3\sigma < 1000''$, but we allowed 20 targets with uncertainties up to $3\sigma = 3000''$ for which we observed two or three nearby fields.
- The O-C residuals for 1,854 NEA measurements show that most measurements are located closely around the origin, with a standard deviation $0.26''$ in α and $0.34''$ in δ.
- We identified 22,000 observations of about 3500 known minor planets (mostly MBAs) and about 10,000 observations of about 1500 unknown objects (most consistent with MBAs), which were measured and reported to the MPC by our team.
- Four new NEAs were discovered serendipitously in the analyzed fields and were then secured with the INT and other telescopes, while two more NEAs were lost due to very fast motion and lack of rapid follow-up time. Nine designated NEAs are discovered by the EURONEAR in 2014 and 2015.
- Three hundred fifteen MPS publications, including data for one-opposition NEAs, were recovered during this project.

Acknowledgements. The PI of this project is indebted to the three TACs (Spanish, British, and Dutch) for granting INT time (ten proposals during five years) in soft-override mode, which was essential to complete this project and secure most discoveries. Special thanks are due to M. Micheli (ESA-SSA), observers P. Ruiz, D. Abreu, and the other TOTAS team (D. Koschny, M. Busch, A. Knöfel, E. Schwab) for the ESA OGS 1 m follow-up of 2015 LT24, 2015 VF65, and the attempt to observe 2015 VG66. Acknowledgements are due to R. Duffard and S. Martin Ruiz (IAA Granada) for granting some time at the Sierra Nevada Observatory (EURONEAR node) with their 1.5 m telescope to secure 2015 LT24 and 2015 VG66. Many thanks to O. Hainaut (ESO) and M. Micheli (ESA) for the VLT astrometry of 2015 HA117 (extremely fast, faint, and close to the South Pole in just a few days), which prolonged its orbit to a seven-day arc. IO acknowledges support from the European Research Council (ERC) in the form of Advanced Grant, COSMICISM. RT acknowledges funding for her La Palma trip to Armagh Observatory, which is core-funded by the Northern Ireland Government. The research led by BTG, CJM, and NPGF has received funding from the European Research Council under the European Union's Seventh Framework Programme (FP/2007-2013) / ERC Grant Agreement n. 320964 (WDTRACER). Thanks are due to the anonymous referee, whose suggestions helped us to improve the paper.

References

Birlan, M. et al., 2010, A&A, 511, 40
Boattini, A. and Forti, G. 2000, P&SS, 48, 939
Erben, T. et al., 2005, AN, 326, 432
Milani, A., 1999, Icarus, 137, 269
Milani, A., 1999, Icarus, 140, 408
Milani, A., 2000, Icarus, 144, 39
Milani, A., 2001, Icarus, 151, 150
Milani, A. and Gronchi, G. F. 2010, Theory of Orbit Determination (Cambridge University Press), Cambridge, UK
Roeser, S. et al., 2010, AJ, 139, 6, 2440
Tatum, J., Balam, D. and Aikman, G. C. L. 1994, P&SS, 42, 611
Schirmer, M., 2013, ApJS, 200, 21
Tichá, J., Tichý, M. and Moravec, Z. 2000, P&SS, 48, 955
Tichá, J., Tichý, M. and Kocer, M. 2002, Icarus, 159, 351
Tichá, J. et al., 2009, M&PS, 44, 1889
Vaduvescu, O. et al., 2008, P&SS, 56, 1913
Vaduvescu, O. et al., 2011, P&SS, 59, 1632
Vaduvescu, O. et al., 2013, P&SS, 85, 299
Vaduvescu, O. et al., 2015, MNRAS, 449, 1614

[1] Isaac Newton Group of Telescopes (ING), Apto. 321, E-38700 Santa Cruz de la Palma, Canary Islands, Spain
[2] Instituto de Astrofísica de Canarias (IAC), C/Vía Láctea s/n, 38205 La Laguna, Tenerife, Spain
[3] Departamento de Astrofísica, Universidad de La Laguna, 38206 La Laguna, Tenerife, Spain
[4] Amateur astronomer, ROASTERR-1 Observatory, 400645 Cluj Napoca, Romania
[5] Unidad de Astronomía, Facultad Ciencias Básicas, Universidad de Antofagasta, Chile
[6] Astronomical Institute of the Romanian Academy, 5 Cutitul de Argint, 040557, Bucharest, Romania
[7] Dpto. de Física Aplicada I, Escuela de Ingeniería de Bilbao, Universidad del País Vasco, Bilbao, Spain
[8] National Solar Observatory, 3665 Discovery Drive, Boulder, CO 80303, USA

[9] Romanian Society for Meteors and Astronomy (SARM), Str. Tineretului 1, 130029 Targoviste, Romania
[10] Amateur Astronomer, Cluj Napoca, Romania
[11] Bucharest Astroclub, B-dul Lascar Catargiu 21, sect 1, Bucharest, 010662, Romania
[12] Institut de Mécanique Céleste et de Calcul des Éphémérides (IMCCE) CNRS-UMR8028, Observatoire de Paris, 77 avenue Denfert-Rochereau, 75014 Paris Cedex, France
[13] Amateur astronomer, Schela Observatory, 800259 Schela, Romania
[14] Faculty of Sciences, University of Craiova, Str. Alexandru Ioan Cuza 13, 200585 Craiova, Romania
[15] Horia Hulubei National Institute for R&D in Physics and Nuclear Engineering (IFIN-HH), Str. Reactorului 30, Magurele, Romania
[16] Armagh Observatory and Planetarium, College Hill, Armagh, BT61 9DG, Northern Ireland
[17] Instituto de Astrofísica e Ciências do Espaço, Universidade do Porto, CAUP, Rua das Estrelas, 4150-762, Porto, Portugal
[18] Nicolaus Copernicus Astronomical Center, Bartycka 18, PL-00-716 Warsaw, Poland
[19] Instituto de Astrofísica de Andalucía (IAA-CSIC), Glorieta de la Astronomía, S/N, Granada, 18008, Spain
[20] Institute for Astronomy, University of Edinburgh, Royal Observatory, Blackford Hill, Edinburgh EH9 3HJ
[21] European Southern Observatory, Karl-Schwarzschild-Str. 2, 85748 Garching, Germany
[22] Qatar Environment and Energy Research Institute (QEERI), HBKU, Qatar Foundation, P.O. Box 5825, Doha, Qatar
[23] Laboratoire d'astrophysique de Bordeaux, Univ. Bordeaux, CNRS, B18N, allée Geoffroy Saint-Hilaire, 33615 Pessac, France
[24] Centro de Astrobiología (INTA-CSIC), Dpto. de Astrofísica, ESAC Campus, Camino bajo del Castillo s/n, 28692 Villanueva de la Cañada, Madrid, Spain
[25] Centre for Astrophysics Research, Science and Technology Research Institute, University of Hertfordshire, College Lane, Hatfield, AL10 9AB, UK
[26] Department of Physics, University of Warwick, Coventry CV4 7AL, UK
[27] Department of Physics and Astronomy, University of Sheffield, Sheffield S3 7RH, UK
[28] Astrophysics Research Centre, School of Mathematics and Physics, Queen's University Belfast, BT7 1NN, UK
[29] School of Physics and Astronomy, University of Nottingham, University Park, Nottingham NG7 2RD, UK
[30] Institute of Astronomy, University of Cambridge, Madingley Road, Cambridge CB3 0HA, UK
[31] UK Astronomy Technology Centre, Blackford Hill, Edinburgh, EH9 3HJ, Scotland
[32] School of Physical Sciences, The Open University, Milton Keynes, MK7 6AA, UK
[33] Institute of Astronomy, University of Cambridge, Cambridge CB3 0HA, UK
[34] Department of Astrophysics/IMAPP, Radboud University, P.O. Box 9010, 6500 GL, Nijmegen, The Netherlands
[35] Kapteyn Astronomical Institute, University of Groningen, Postbus 800, NL-9700 AV Groningen, the Netherlands
[36] Leiden Observatory, Leiden University, PO Box 9513, NL-2300 RA Leiden, the Netherlands
[37] Department for Geophysics, Astrophysics and Meteorology, Institute of Physics, NAWI Graz, Universitätsplatz 5, A-8010 Graz, Austria
[38] Instituto de Astrofísica e Ciências do Espaço, Faculdade de Ciências da Universidade de Lisboa, Portugal
[39] The University of Hong Kong, Department of Physics, Hong Kong SAR, China
[40] The Laboratory for Space Research, The University of Hong Kong, SAR, China
[41] Institute of Astronomy and Department of Physics, National Tsing Hua University, Hsinchu 30013, Taiwan

Table 2. 368 NEAs targeted in 453 fields during this project. We explain the columns in Sect. 2.3.

NEA	Obs Date	V	μ	3σ	Imgs	TEXP	Status	MPS	Comments
1999DB2	20150614	23.2	0.4	277	8	90	NOTF		
...	20150818	22.6	0.7	388	12	90	RECO	621143	
1999JO6	20150114	22.8	0.3	132	6	120	REC	561149	
2000GV127	20140321	23.1	0.9	358	8	120	NOTFY		
2000WY28	20140408	23.2	0.8	520	10	120	REC	511076	TS
2001AV43	20130907	22.0	0.4	571	5	180	REC	476154	
2001EC16	20150114	22.6	0.8	31	4	120	REC	561150	
2001FZ	20160329	23.2	0.8	763	2	90	NOTFY		
2001GM2	20130907	22.6	0.4	357	5	180	REC	476155	
2001HW7	20140601	23.0	2.2	656	10	120	NOTF		G96 20170318
...	20140921	23.0	0.7	665	8	90	NOTF		
2001NJ6	20140921	22.9	0.6	423	8	90	RECR	806513	T08 20170718
2001QB34	20140526	21.7	0.4	468	6	120	RECR	766112	J04 20140529
2001QE34	20140731	23.1	0.3	838	6	120	REC	758947	
2003QF70	20130927	22.1	1.7	176	6	120	NOTF		H21 20131128
2001RX17	20150114	23.4	0.6	226	8	120	NOTFY		
2001UP16	20140709	23.1	0.6	700	8	120	NOTFY		
...	20140728	22.8	0.8	752	6	120	NOTFY		
2002CV46	20140827	22.3	2.1	993	6	60	NOTF		
...	20140830	22.6	2.1	993	8	60	RECO	529735	TS
2002EX8	20150114	22.7	0.6	137	6	120	REC	762144	TS
2002GA	20151228	23.4	0.4	647	10	90	RECO	665447	
...	20160101	23.4	0.4	647	15	90	RECO	665447	TS
2002ON4	20150131	22.8	1.7	241	8	120	NOTF		
...	20150429	21.7	2.1	375	6	90	REC	603194	
2002PQ6	20140526	23.7	0.7	278	10	150	NOTFY		
2002RP28	20160310	22.4	1.2	757	6	60	NOTF		
...	20160329	22.8	0.9	716	6	90	RECO	695963	TS
2002SL	20150225	22.6	0.7	781	6	100	NOTF		
...	20150226	22.6	0.7	781	6	100	REC	583273	
...	20150228	22.6	0.7	781	6	120	REC	583273	
2002TS69	20160824	23.4	1.1	614	8	60	RECO	725060	WHT
2002VT94	20140321	23.1	0.6	1041	6	120	NOTFY		
2003QR79	20140222	21.6	4.2	54	6	45	RECJ	502319	291 20140220
2003TK2	20140901	23.4	1.1	597	8	90	NOTF		PHA
...	20140922	23.6	0.8	511	8	120	RECO	772053	
...	20141222	23.0	0.9	983	2x6	120	RECO	772053	
2003WU153	20150423	23.0	0.9	1437	6	120	REC	606384	
...	20150510	23.0	0.9	1401	2x6	120	REC	606384	
2004CL1	20141103	23.0	0.6	313	6	120	REC	544285	
2004FZ5	20140923	22.9	0.8	288	8	120	RECO	536595	
2004PE20	20140601	22.8	2.2	506	6	120	NOTF		
...	20140602	22.8	2.2	506	12	120	REC	517904	
2004RW10	20150821	23.3	0.3	501	8	90	RECO	645358	PHA
...	20151105	23.4	0.8	914	2x10	60	RECO	645358	TS
2005DO	20130907	22.9	0.9	711	5	150	NOTFY		
2005EQ70	20160329	22.4	1.5	747	8	60	NOTFY		
...	20160526	22.7	2.2	954	2x6	60	NOTFY		
2005EZ	20160419	22.4	0.3	431	6	60	NOTFY		
2005FV2	20150510	22.7	0.9	728	6	120	NOTFY		
2005JF46	20140220	22.3	1.8	1515	6	90	NOTFY		
2005LV3	20150528	22.3	1.7	1000	6	60	NOTF		
...	20150614	22.2	1.4	292	6	60	NOTF		
...	20150818	21.9	0.3	378	6	60	NOTF		
...	20150821	21.9	0.3	378	8	90	REC	623287	
2005NY39	20150421	22.9	0.8	793	8	120	RECO	600694	
2005QF88	20150528	22.8	0.7	3000	6	90	NOTFY		
...	20151101	23.0	2.2	916	6	60	NOTFY		

Table 2. continued.

NEA	Obs Date	V	μ	3σ	Imgs	TEXP	Status	MPS	Comments
...	20151210	23.2	2.4	976	2x6	60	NOTFY		
...	20151212	23.2	2.4	976	2x8	60	NOTFY		
2005QL76	20150822	22.4	2.2	294	6	60	REC	623287	
...	20150823	22.4	2.2	294	6	60	REC	623287	
2005QO11	20140223	22.1	1.3	1330	6	90	RECO	502328	
2005SW4	20140831	22.5	2.1	356	8	90	REC	529759	
2005SX4	20140728	22.8	0.9	814	6	120	NOTF		F51 20140827
2005TF	20130801	22.4	0.9	181	7	120	NOTF		H36 20160831
2005UJ1	20160419	23.1	0.6	800	8	90	NOTFY		
2005UP64	20140921	22.4	1.5	848	6	60	REC	533199	
2005YA37	20151013	22.4	1.3	525	6	60	RECO	631343	
2005YT55	20160329	23.0	2.0	911	2x6	90	RECO	695971	TS
2006AM8	20160329	23.0	0.6	786	2x6	90	REC	695971	TS
2006BX139	20140603	22.9	2.3	404	8	120	NOTF		807 20131105
2006CL10	20150117	22.8	3.6	384	8	90	RECO	562595	TS
2006CL9	20140728	23.0	1.2	832	8	100	NOTFY		
2006CV9	20141103	21.8	1.3	908	6	90	REC	544828	
2006FG36	20151013	22.2	0.8	266	5	60	NOTF		
...	20151103	22.1	0.9	262	8	60	RECO	642148	TS
2006GT3	20150128	22.4	0.5	1187	2x6	90	REC	567503	
2006HC2	20150225	22.6	2.0	721	6	100	NOTF		PHA 568 20150910
...	20150226	22.6	2.0	721	6	100	NOTF		
...	20150228	22.6	2.0	721	2x6	100	NOTF		
2006KL89	20150114	21.8	0.7	972	2x5	60	NOTF		J04 20160212
2006MA	20150823	22.8	1.0	110	6	90	NOTF		568 20151013
2006OF5	20150423	22.3	0.4	693	6	90	NOTF		926 20150521
2006OV5	20150821	22.8	1.0	241	6	90	REC	623291	
2006SS19	20150510	22.5	0.2	888	8	90	RECJ	623293	695 20150217
2006TD1	20150129	23.0	0.2	329	12	90	NOTF		
...	20150225	22.6	0.9	404	6	100	RECO	583294	TS
...	20150226	22.6	0.9	404	6	100	RECO	583294	
2006UM	20140623	22.6	0.5	24	6	120	REC	520013	
2006VX2	20151103	22.8	3.9	838	2x8	60	RECO	642157	
2006VY2	20161017	22.7	2.2	878	8	90	NOTFY		
2006XJ1	20130626	20.4	2.3	932	8	60	REC	474946	
...	20130801	21.4	1.0	768	6	120	REC	474946	
2007CS26	20140509	22.7	2.9	838	6	120	NOTFY		PHA
...	20140526	22.8	2.9	850	12	90	NOTFY		
2007EK88	20140728	23.1	0.8	153	6	120	RECO	523705	
2007EY	20140509	22.2	2.7	1100	6	120	RECR	762176	TS
2007EZ	20140623	23.4	0.7	190	8	150	NOTF		J04 20150811
2007FH1	20140731	22.8	0.4	358	6	120	REC	523706	
2007GU4	20140827	23.2	1.2	892	6	120	NOTFY		
2007GZ5	20140223	22.1	1.2	104	6	90	NOTF		926 20160925
...	20140320	22.2	1.1	90	6	120	NOTF		
...	20140623	23.4	1.6	51	8	120	NOTF		
...	20160419	22.4	3.0	129	6	60	NOTF		
2007PQ9	20150128	22.8	1.3	78	6	90	NOTF		TS
...	20150129	22.8	1.3	78	12	90	RECO	569601	TS
...	20150131	22.8	1.3	78	10	60	RECO	569601	WHT
2007PV27	20150311	21.7	4.1	38	10	40	NOTF		PHA OGS 291 20150315
...	20150312	21.7	4.1	38	10	40	NOTF		OGS
2007RD1	20140728	22.8	0.4	511	8	120	RECO	526531	TS
2007TG15	20140921	22.3	2.2	210	6	60	REC	533236	
2007UW3	20151101	22.3	1.5	394	6	60	RECR	775904	
...	20151102	22.3	1.5	395	12	60	RECR	775904	
...	20151129	22.3	1.8	458	8	60	RECO	653534	
2007WF55	20140728	23.4	0.4	166	8	120	RECO	527075	TS
2007WU3	20140917	23.2	0.6	927	8	120	NOTF		926 20150707

Table 2. continued.

NEA	Obs Date	V	μ	3σ	Imgs	TEXP	Status	MPS	Comments
2007XJ16	20140922	23.3	1.0	279	8	120	REC	560035	PHA
...	20141225	22.8	0.7	402	6	120	REC	560035	TS
2007XP3	20140223	21.5	1.4	1208	6	90	REC	502363	
2008CH	20140728	23.5	1.0	341	8	120	REC	523730	PHA
2008CL72	20150128	22.9	2.3	214	6	90	NOTF		
...	20150131	21.9	2.3	214	8	60	REC	569602	
2008DC	20150821	21.5	2.9	727	6	60	NOTF		G45 20160216
...	20150823	21.5	2.9	727	2x4	60	RECR	762185	
2008DL5	20140526	23.2	1.5	795	8	120	REC	516487	
2008EJ	20140220	21.8	1.8	1283	8	90	REC	501628	
2008EN6	20150114	22.5	0.7	330	8	90	REC	561186	
2008GJ	20151101	23.2	0.6	640	6	90	NOTF		
...	20151228	23.1	1.7	605	8	80	NOTF		
...	20151230	23.1	1.7	605	10	60	RECO	663955	
2008GP20	20151013	21.8	1.4	939	2x6	60	RECO	631400	
2008GS3	20160419	22.6	3.8	869	6	60	NOTFY		
2008GX	20150117	22.7	1.5	513	6	90	REC	567539	
2008HE66	20130801	22.1	0.4	148	6	120	RECJ	473028	568 20130714
2008JJ	20150131	22.8	1.4	947	8	120	NOTF		926 20150419
2008KQ	20150128	22.7	1.0	232	6	90	RECO	567541	
2008ON	20151129	22.5	1.8	902	8	60	NOTF		
...	20151210	22.8	1.8	902	6	60	NOTF		
...	20151228	23.0	1.8	609	8	60	RECO	665500	TS
...	20151230	23.0	1.8	609	10	60	RECO	665500	TS
...	20160101	23.0	1.8	609	15	90	RECO	665500	TS
...	20160103	23.0	1.8	587	2x8	90	RECO	665500	TS
2008PG2	20140220	21.9	1.7	919	6	90	RECO	501629	
2008PL3	20150528	22.0	2.1	600	6	60	REC	608608	
2008QC	20151120	22.7	1.0	694	2x6	60	RECO	650646	
2008RS26	20130801	21.8	0.7	161	5	150	NOTF		568 20130715
2008SE	20150614	22.0	0.8	204	6	60	REC	611552	
2008TN26	20130907	21.9	0.2	304	5	120	REC	476280	
2008TR2	20140408	22.4	1.3	477	10	120	RECO	509807	TS
2008UW91	20140923	23.2	1.4	696	8	120	REC	536671	PHA
2008WK	20130907	22.9	1.2	317	6	120	RECR	734336	TS
2008YE3	20150422	23.0	1.1	257	6	120	RECO	600728	
2009AS	20141031	22.5	0.7	880	6	90	NOTF		F51 20160801
2009BB	20151202	23.3	0.8	506	10	90	RECO	653544	
2009CR4	20160110	22.4	1.1	999	6	60	REC	668453	
2009DG9	20140222	22.3	1.4	717	6	150	RECO	502383	
2009EC	20140731	22.5	0.7	85	6	120	REC	523750	
2009HW44	20140831	21.9	1.2	305	6	90	REC	529818	
2009JG1	20140320	22.6	0.8	293	8	120	RECO	506429	
2009LX	20140731	22.9	1.2	79	6	120	RECO	523753	
2009QH2	20160825	23.5	1.2	174	8	60	NOTFY		WHT
2009QZ34	20160825	23.3	0.5	757	8	60	NOTFY		WHT
2009RN	20141002	22.9	1.9	83	6	90	RECO	538930	
2009SG18	20140526	23.3	6.2	778	12	45	RECO	516505	PHA
2009SQ172	20130626	21.5	0.3	322	10	180	REC	472651	
2009SV	20140222	21.4	1.5	1543	6	90	NOTF		
...	20140319	21.3	2.3	1195	4x6	60	REC	506431	
2009SV171	20130907	23.0	0.8	72	3	90	NOTF		568 20130911
2009TL4	20140827	22.0	0.3	658	6	90	NOTF		
...	20140830	22.0	0.3	658	8	90	RECO	553174	
...	20141215	22.8	2.5	659	3x8	60	RECO	553174	TS
2009TM10	20130927	22.1	2.0	250	6	90	NOTF		926 20140126
2009UD2	20141001	22.3	2.5	175	6	60	RECO	536685	
2009UW2	20130801	22.1	2.2	351	6	60	NOTF		H21 20130903
...	20130907	21.2	3.6	488	5	30	RECR	476311	

Table 2. continued.

NEA	Obs Date	V	μ	3σ	Imgs	TEXP	Status	MPS	Comments
2010BH2	20140602	22.9	0.7	60	4	120	NOTF		807 20161027
2010CH55	20140803	22.3	2.4	608	8	120	REC	525572	
2010CN44	20140901	23.0	1.7	330	6	90	RECR	791066	PHA TS 568 20141021
...	20140917	22.4	2.0	478	10	90	RECR	791066	TS
2010DH77	20160107	21.5	2.0	977	2x6	60	REC	665520	
2010DM21	20140728	23.3	1.4	156	6	120	REC	528170	
2010FR	20140623	23.3	1.4	262	8	150	REC	520038	PHA
2010GA7	20160527	23.2	2.2	231	8	60	NOTF		568 20160511
2010HG20	20151210	22.7	2.2	344	6	60	NOTF		
...	20151212	22.7	2.2	799	2x8	60	REC	659816	TS
2010HX107	20150421	22.3	4.1	339	10	60	REC	600740	
2010JF87	20130907	22.9	1.6	970	5	120	REC	476327	
2010JG87	20140728	21.9	1.2	731	8	120	REC	523769	
2010JH88	20140623	23.0	0.7	295	9	150	REC	781950	
2010MH1	20151228	23.0	1.5	471	8	60	NOTF		G96 20160704
...	20151230	23.0	1.5	471	10	60	RECR	739867	TS
2010MP1	20140531	21.5	2.4	988	10	90	RECO	519383	
2010MR	20140531	20.6	0.3	659	7	120	NOTF		675 20140529
2010MW1	20140526	21.4	1.3	91	6	120	REC	516512	
2010OC127	20140608	22.3	2.2	323	6	120	RECR	766157	TS
...	20140731	22.0	2.2	293	6	60	REC	523772	
2010OQ1	20130626	21.1	0.9	38	6	120	RECR	474396	568 20130715
2010PR66	20150114	22.5	0.6	287	6	120	REC	561206	PHA
2010RB	20140728	22.7	1.0	130	6	120	REC	523772	
2010RN82	20140623	22.8	0.7	66	8	150	RECO	520043	
2010RS180	20150421	21.7	1.0	399	6	60	REC	600741	
2010SH13	20140709	23.2	1.1	131	6	120	RECJ	522816	PHA 695 20140618
2010TU149	20140623	22.5	1.8	12	8	120	RECJ	520044	PHA 568 20140621
2010TX54	20150225	22.8	1.2	773	8	90	RECO	583334	TS
2010UE7	20150114	22.8	0.4	132	6	120	REC	562717	
2010UK8	20140509	21.7	3.8	537	6	120	NOTF		PHA 568 20150725
2010VC72	20151107	22.1	1.5	872	2x6	60	REC	645454	
2010VD72	20160824	23.2	2.7	195	16	30	RECO	725066	PHA WHT TS
2010VX39	20160310	22.6	0.2	53	8	60	REC	692678	TS
2010VY139	20140728	23.3	0.8	559	6	120	NOTFY		
...	20140917	23.1	0.4	482	8	120	NOTFY		
...	20150201	22.8	2.5	669	6	80	NOTFY		
2010VZ	20140602	22.8	1.6	240	6	120	REC	517944	PHA
2010WH	20150117	22.4	1.1	151	6	90	REC	562723	TS
2010WQ7	20150429	22.0	0.2	14	6	90	REC	603244	
2010XQ69	20160107	21.3	3.0	731	2x6	60	REC	668473	
2010XY72	20141103	21.6	1.7	250	6	60	REC	544308	PHA
2010XZ	20160112	22.2	3.0	262	6	60	RECO	668472	TS
2010XZ67	20130907	21.0	1.0	160	4	90	RECJ	476342	033 20130905
2010YB	20150614	23.3	1.3	462	8	90	NOTF		PHA J04 20150715
2011AF37	20140526	23.0	0.8	146	6	120	RECO	516519	
2011AH37	20140623	22.9	0.4	145	6	150	REC	520046	PHA
2011AM24	20150114	22.5	1.4	73	6	90	REC	561212	PHA TS
2011AN16	20160419	22.5	0.4	80	6	60	NOTF		705 20160502
2011BD40	20130626	21.2	1.7	630	6	150	NOTF		I41 20130801
2011BF59	20150822	22.7	0.2	526	8	60	RECR	767259	TS
...	20151013	20.8	1.8	776	2x6	60	REC	631466	
2011BO59	20160107	22.0	2.0	703	2x6	60	RECJ	665532	PHA J04 20160107
2011CG2	20150822	23.5	1.2	12	6	90	REC	623309	PHA TS
2011ET4	20140917	22.9	1.5	637	8	120	REC	533316	
2011EU29	20140709	22.7	0.6	543	6	120	NOTF		PHA
...	20140728	21.6	1.0	618	8	90	RECJ	523793	568 20130715
2011EW29	20141215	22.7	0.9	547	6	120	RECO	553219	
2011GA62	20151107	23.0	0.7	98	8	60	RECR	645462	568 20140307

Table 2. continued.

NEA	Obs Date	V	μ	3σ	Imgs	TEXP	Status	MPS	Comments
2011GE2	20160116	22.4	0.8	989	8	60	NOTF		F51 20160211
...	20160117	22.4	0.8	989	2x6	60	NOTF		
2011GL60	20140728	23.3	0.9	100	6	120	RECO	523793	
2011GO27	20140623	23.2	0.5	579	8	120	RECR	766164	TS
2011GP59	20150128	22.7	2.9	480	6	120	RECO	567618	TS
2011HE24	20160104	23.2	0.7	381	12	90	RECO	665539	
2011JA8	20160310	22.9	0.6	22	6	60	NOTF		
...	20160329	23.0	0.6	21	6	60	RECO	696002	
2011JT9	20150114	22.6	0.3	93	6	120	REC	561221	
2011KO17	20150818	23.3	0.8	135	6	90	RECO	621210	PHA TS
2011LA19	20160310	22.5	0.6	270	6	60	REC	692693	PHA
2011LH	20151228	23.1	1.0	375	8	80	NOTF		
...	20160103	23.1	1.0	375	8	90	RECO	665540	
...	20160105	23.1	1.0	375	10	90	RECO	665540	
2011MD11	20140326	23.0	0.6	34	8	120	REC	508606	
2011ME5	20150128	22.7	1.2	18	6	90	REC	567625	
2011MK	20140326	21.6	0.5	180	8	90	REC	506469	
2011OC18	20140526	21.7	0.6	445	12	120	REC	516520	
2011OL5	20141001	22.3	1.6	66	6	90	REC	536724	
2011PO1	20150528	23.3	1.2	935	8	120	RECR	762215	PHA TS 568 20150522
2011PT	20140623	22.9	0.6	249	8	120	REC	520047	
2011PU	20140526	22.2	0.7	478	6	120	REC	516521	
2011PU1	20140508	23.8	0.4	1000	3x7	120	NOTF		VI 568 20140404
2011QH21	20140531	22.0	1.3	15	8	150	REC	519385	
2011QZ13	20141001	22.6	2.0	40	6	75	RECO	536725	
2011SB25	20130907	22.5	2.5	404	5	90	RECO	476356	TS
2011SJ68	20140623	23.0	0.7	30	8	150	RECO	520048	
2011SO26	20150818	22.9	1.0	68	6	90	RECO	621214	
2011SP68	20140326	22.6	0.7	482	8	120	RECO	506475	
2011SR12	20140222	22.0	0.3	1405	6	120	NOTF		F51 20170112
2011SR69	20160329	22.9	0.9	47	6	60	REC	696003	TS
2011UA	20140321	22.8	0.6	191	6	120	RECO	665545	TS
...	20160104	22.7	0.7	279	12	60	RECO	665545	
2011UA131	20150821	21.3	0.6	487	6	60	NOTF		
...	20150823	21.3	0.6	487	2x4	60	REC	623313	
2011UD256	20130927	22.4	2.4	117	6	90	NOTF		568 20140826
2011UF21	20130907	22.6	0.7	495	5	180	RECO	476358	
2011UV63	20151120	21.4	1.4	567	8	60	REC	650674	PHA
2011VH5	20141002	22.9	0.7	165	6	120	REC	538955	
2011VR5	20150822	23.2	0.5	170	6	90	RECR	794827	TS
...	20151105	21.0	0.8	320	6	60	REC	642204	
2011WE44	20140827	23.5	0.8	396	6	120	NOTF		
...	20140830	23.4	0.8	396	8	120	RECO	529861	
2011WH15	20141031	22.7	1.2	752	6	90	RECO	544310	TS
2011WK15	20141002	22.9	1.0	183	6	120	REC	538955	
2011XA3	20151202	23.5	1.4	791	10	90	RECO	653571	PHA TS
2011XE1	20140917	22.8	0.6	13	8	120	REC	531548	
2011YT62	20160110	22.5	0.4	350	6	60	REC	668492	
2011YW1	20150614	22.6	1.1	90	6	90	NOTF		J04 20161129
2012AC13	20140728	21.9	0.7	176	6	120	RECJ	523813	568 20140725
2012AD3	20140526	22.9	0.9	165	6	120	REC	516535	PHA
2012AY	20151202	23.0	1.4	15	8	90	RECJ	653573	705 20151202
2012BB2	20130801	22.1	1.0	84	6	120	NOTF		568 20130808
2012BD27	20160110	22.2	2.9	83	6	60	RECO	668494	
2012BJ134	20150128	22.6	0.9	120	8	90	RECJ	567628	TS 568 20150117
2012CM29	20150429	22.8	0.2	178	8	90	RECJ	604641	568 20160429
2012DE61	20140728	22.8	0.2	524	6	120	RECO	523826	
2012DJ4	20130801	22.7	0.8	64	9	180	NOTF		568 20130715
2012DH4	20150128	22.8	3.7	9	8	90	RECR	762231	TS 568 20150917

Table 2. continued.

NEA	Obs Date	V	μ	3σ	Imgs	TEXP	Status	MPS	Comments
2012DH61	20141215	22.2	0.9	27	6	120	RECO	553229	
2012DN	20140526	21.7	0.6	515	6	120	REC	516536	
2012EL5	20150822	22.6	1.4	788	6	60	NOTF		
...	20150823	22.6	1.4	788	2x6	60	REC	623316	
2012FH38	20140220	22.3	1.2	663	9	120	RECR		PHA F51 20170730
2012FO62	20140901	22.9	2.6	467	6	90	NOTF		PHA
...	20140922	22.6	2.9	528	6	60	REC	533337	
2012FP62	20140917	21.7	2.1	821	8	90	REC	531558	
2012FR62	20130927	21.4	2.3	166	6	90	RECJ	478855	033 20130927
2012GV17	20140322	22.9	1.1	17	8	120	RECO	506487	PHA
2012HB34	20150510	23.0	1.0	856	6	120	NOTFY		
2012HN2	20151107	22.7	0.8	669	2x8	60	REC	645501	
2012HO15	20160310	21.7	3.0	32	6	60	REC	690243	
2012HO2	20150614	22.4	1.3	763	6	60	REC	642211	
...	20151101	22.8	1.8	277	6	60	NOTF		
...	20151102	22.8	1.8	280	12	60	REC	642211	TS
2012HP13	20140408	24.0	5.0	217	15	80	NOTF		VI 309 20140409
2012HS15	20150420	22.2	0.9	474	6	60	RECJ	600757	H21 20150417
2012HZ33	20160118	22.6	1.6	7	6	60	REC	671888	WHT PHA
2012KJ18	20150228	22.6	0.4	72	6	120	REC	583355	
2012KK18	20160329	23.2	0.5	44	6	90	RECO	696011	
2012KL45	20140220	21.6	1.0	18	6	120	RECJ	501641	291 20140209
2012KM45	20141225	23.1	0.8	12	8	120	RECO	558854	
2012KY41	20140223	22.3	0.7	76	6	150	REC	502419	
2012LE11	20160329	23.2	0.6	12	6	90	RECO	696011	
2012MG7	20140605	22.3	1.3	403	8	120	REC	518841	
2012MQ	20150510	23.2	1.0	168	8	120	RECO	606412	TS
2012MR7	20140531	21.8	0.7	75	7	120	NOTF		
...	20140601	21.8	0.7	75	6	120	REC	519387	
2012MS6	20160329	22.9	0.6	55	6	60	RECO	696011	
2012NP	20150510	21.5	0.8	757	6	90	NOTF		926 20150519
2012OA1	20150420	22.5	1.0	1127	6	90	NOTF		
...	20150510	22.6	0.6	175	6	120	RECO	607316	
2012OE1	20150422	22.5	0.8	383	6	90	RECO	600758	
2012OU5	20150510	22.9	0.6	496	6	120	NOTFY		
...	20150528	22.4	0.7	2639	6	60	NOTFY		
2012PC20	20150114	22.6	0.8	194	6	120	REC	561244	
2012PJ6	20150422	22.9	0.6	325	6	120	RECO	600758	TS
2012PQ28	20150614	22.2	0.6	9	6	60	RECO	611571	
2012QG8	20160112	22.2	2.1	975	6	60	REC	668506	TS
2012QR50	20140731	22.2	1.9	38	6	120	REC	523829	
2012SA59	20160828	23.1	0.2	18	6	90	NOTFY		WHT
...	20160829	23.1	0.2	18	10	90	NOTFY		
2012SK8	20150128	22.5	0.3	97	6	90	NOTF		J04 20150212
2012SL8	20150822	22.9	0.9	89	6	60	REC	623317	
2012SN30	20140831	22.4	1.7	51	6	90	REC	529878	
2012SW20	20160117	22.8	0.9	350	8	60	REC	671891	PHA TS
2012TA79	20150422	22.9	0.4	103	6	120	REC	600762	TS
2012TO139	20151228	22.8	1.3	539	8	60	NOTF		PHA
...	20160103	22.9	1.3	468	8	90	REC	665571	
...	20160105	23.0	1.3	419	10	90	REC	665571	
2012TS78	20140709	22.6	0.6	29	8	120	REC	522819	PHA
2012TU	20140220	21.9	1.1	1499	6	120	NOTF		RECR 926 20140327
2012TZ52	20140728	22.3	0.9	59	8	120	REC	523829	
2012UP27	20140526	21.1	1.4	127	6	120	REC	516538	
2012US68	20151228	22.5	0.9	302	6	80	NOTF		
...	20160103	22.5	0.9	302	8	90	REC	665572	
2012UW136	20130927	21.3	2.8	290	6	60	REC	478860	
2012VF5	20140322	22.5	0.8	129	8	120	REC	506515	

Table 2. continued.

NEA	Obs Date	V	μ	3σ	Imgs	TEXP	Status	MPS	Comments
2012VF80	20140322	22.7	0.6	36	8	120	REC	506517	TS
2012XC55	20150814	22.4	0.9	127	6	90	REC	621231	
2012XE112	20151013	22.4	0.8	126	5	60	REC	631525	
2012XH16	20141031	22.9	1.1	103	6	120	NOTFY		
2012XO111	20160117	22.9	2.9	120	6	60	NOTF		PHA
...	20160118	22.9	2.6	120	6	60	RECO	671891	WHT TS
2012XQ93	20140608	22.2	0.5	885	6	120	NOTF		F51 20140703
2012XS111	20141103	20.3	4.2	556	6	40	REC	544858	PHA
2012YN6	20151105	23.5	1.0	316	10	60	RECO	645505	TS
2012YY6	20160526	22.8	1.0	690	8	60	NOTF		PHA 568 20160529
2013AA53	20150114	22.0	1.4	186	6	90	REC	561247	
2013AE69	20140917	22.2	1.1	146	12	120	RECO	531560	
2013AW60	20140526	22.4	0.6	24	6	120	RECR	766187	291 20140618
2013BF27	20151013	22.8	1.1	17	10	60	REC	631529	
2013BO73	20150128	22.9	0.7	53	6	120	RECJ	567642	PHA 568 20150117
2013BP45	20140408	22.7	2.1	976	8	120	RECO	509857	
2013BW76	20140526	23.0	0.8	25	6	120	NOTF		PHA 568 20140620
...	20140603	23.0	0.7	20	8	120	NOTF		
2013CJ89	20140220	21.8	3.3	1925	6	60	NOTF		807 20160121
...	20150228	22.7	1.4	685	6	120	NOTF		
2013CK89	20150614	22.6	0.6	127	6	90	REC	611580	
2013CN129	20140220	21.5	3.3	229	8	40	REC	501647	
2013CN35	20141002	22.6	2.0	145	6	90	NOTF		
...	20141103	21.9	2.4	204	6	90	RECO	544312	
2013CP35	20160823	22.4	0.4	40	8	90	RECO	725072	WHT
2013CU83	20160117	22.7	0.5	402	8	60	RECJ	671892	PHA 807 20160116
2013EC28	20140917	22.7	1.0	108	14	120	REC	533347	TS
2013EW27	20140728	23.1	0.6	7	6	120	REC	523847	PHA
2013GH84	20150114	22.7	2.1	32	6	120	RECO	561248	PHA
2013GU68	20150128	22.6	0.6	267	6	90	REC	567642	
2013GW68	20140319	21.7	6.7	220	8	40	REC	506541	
2013GY7	20160310	22.6	2.7	5	8	60	RECO	692716	PHA
2013JX2	20141225	22.6	0.8	144	6	120	RECO	558862	
2013JY35	20140605	22.6	1.3	386	8	120	REC	518845	
2013JZ28	20160527	23.1	0.5	276	8	60	NOTFY		
2013KN6	20140623	22.4	1.0	40	8	120	NOTF		PHA 568 20140620
2013LF1	20160527	23.2	0.6	156	8	60	NOTFY		
2013LK31	20160526	22.7	1.0	544	6	60	NOTFY		
2013LV28	20140831	22.2	1.4	18	6	90	REC	529895	
2013LX28	20140526	21.8	3.4	348	8	90	REC	516555	
2013MR	20140728	22.8	3.3	41	6	60	RECJ	523876	568 20140725
2013MS11	20141222	22.4	1.1	164	6	90	RECO	558866	TS
2013MW6	20141031	22.7	1.0	589	12	90	RECO	544313	
2013MZ5	20150528	22.1	1.7	2179	6	60	REC	608663	
2013NJ10	20150429	22.5	0.2	106	8	90	REC	603275	PHA
2013NJ15	20150814	22.7	1.8	442	6	90	RECO	621238	
2013NK4	20140526	21.0	0.7	69	6	120	RECJ	516555	PHA J04 20140526
2013OS3	20140731	23.2	1.0	56	6	120	REC	523876	
2013PF10	20151101	23.1	0.4	940	6	90	NOTFY		
...	20151103	23.2	0.4	930	8	60	NOTFY		
2013PY38	20140623	23.1	2.0	504	8	120	NOTF		
...	20150423	22.4	2.3	1491	6	90	RECO	608663	
2013QC11	20141215	22.4	1.5	161	6	90	NOTF		PHA 568 20141125
2013QK48	20140901	22.8	0.5	205	6	90	REC	531574	PHA
2013QN10	20140831	22.5	1.8	53	2x6	90	RECJ	529896	568 20140827
2013RC21	20140728	21.1	4.9	479	6	30	REC	523877	
2013RU5	20140623	23.0	0.8	450	8	150	RECO	520073	
2013RX80	20150814	22.2	0.8	450	6	90	RECO	621238	
2013SR24	20150420	23.2	0.6	254	8	120	NOTF		T12 20170225

Table 2. continued.

NEA	Obs Date	V	μ	3σ	Imgs	TEXP	Status	MPS	Comments
2013SS19	20140728	23.3	1.3	99	6	120	REC	523877	
2013TC136	20160526	22.7	0.6	106	6	60	NOTFY		
2013TS5	20140728	22.5	0.2	63	6	120	REC	523877	
2013TV144	20150421	22.4	0.9	102	6	90	RECJ	600776	W84 20150421
2013UP8	20140901	23.0	0.1	15	6	90	REC	529896	PHA
2013UX14	20160415	22.7	0.4	17	4	60	RECO	703773	
2013VG13	20140917	22.4	0.9	108	8	120	REC	531574	
2013VM4	20150814	22.3	0.8	42	6	90	REC	621238	
2013VQ4	20140728	22.2	0.8	90	4	120	RECJ	523878	568 20140725
2013WU44	20160112	22.5	3.1	9	12	60	RECO	668520	TS
2013XE22	20150423	22.8	0.1	623	8	120	NOTF		H21 20150512
...	20150510	22.1	0.6	100	6	90	NOTF		
2013XH4	20150818	22.9	0.8	12	6	60	RECO	621238	
2013XS3	20140728	21.4	4.0	84	6	30	REC	523878	
2013YM70	20160112	22.5	2.9	3	6	60	REC	668520	TS
2013YT102	20141215	22.8	3.6	656	10	45	NOTF		
...	20141222	22.8	4.0	570	6	50	RECO	558878	TS
2014AB29	20160828	22.4	1.2	399	8	60	REC	725658	WHT
2014BG3	20141001	22.3	1.3	40	8	90	REC	536760	
2014BH3	20160329	23.0	2.3	421	6	90	NOTFY		
2014BY32	20160116	21.8	1.4	886	16	60	RECJ	671901	926 20160115
2014EA4	20150311	21.7	3.3	90	10	40	RECO	585715	OGS TS
...	20150312	21.7	3.3	90	10	40	RECO	585715	OGS TS
2014HM123	20160104	22.2	1.4	395	8	90	RECO	665592	
2014JG78	20150228	22.0	1.0	20	6	100	REC	583376	
2014JM25	20160419	21.7	0.3	700	5	60	RECR	758963	926 20160429
2014OE338	20150614	22.2	0.2	244	6	60	REC	611588	
2014PB58	20150420	23.0	1.9	1278	10	90	RECO	600788	
2014QX390	20150510	23.1	2.0	10	8	60	NOTFY		
2014RZ11	20160329	22.6	1.0	575	6	60	RECO	696025	
2014SM143	20160526	22.2	3.9	4	8	40	RECO	712041	PHA
2014UH175	20160310	22.9	1.0	397	8	60	RECO	692746	TS
2014VU1	20160329	22.6	0.5	902	6	60	NOTFY		
...	20160527	22.7	0.6	841	2x6	60	NOTFY		
2014WE365	20150821	22.8	0.9	78	6	90	RECO	623329	PHA
2014WS365	20151103	22.7	1.9	770	6	60	RECO	642234	
2014XL7	20160329	23.2	1.1	144	6	90	REC	696036	
2015BJ514	20151129	22.1	0.8	12	6	60	RECO	653606	
2015BO510	20151013	22.7	0.4	4	15	60	RECO	631587	TS
2015FN118	20160823	22.7	1.1	67	8	60	REC	725074	PHA WHT
2015JA2	20160118	23.0	1.3	9	6	60	REC	671927	PHA WHT
2015KX121	20151228	22.8	3.1	83	8	60	NOTF		
...	20151230	22.8	3.1	83	10	60	RECO	663984	
2015MO66	20160329	22.6	1.2	90	6	60	RECJ	696041	705 20160327
2015OB22	20160310	22.5	1.3	375	6	60	REC	692766	